

THE EFFECT OF DIFFERENT BRANDS OF WELDING ELECTRODE ON THE MECHANICAL PROPERTIES OF WELDED JOINTS IN MILD STEEL

M. PITA¹ & M. MAUMELA²

¹Department of Mechanical and Industrial Engineering, Faculty of Engineering and Technology, University of South Africa

²Physical Metallurgy Group, Advanced Materials Division, Mintek, Private Bag X3015, Randburg, South Africa

ABSTRACT

Welding is the process of joining two pieces of similar metals or alloys by fusion. Mild steel is one of the materials most joined using welding techniques. The welding electrode used can influence the mechanical properties of mild steel during the welding process. This paper aims at investigating the effect of electrode brand on the mechanical properties of mild steel during arc welding. The welding method used in this study was shielded metal arc welding (SMAW) with using 3.2 mm electrodes (E6013) of two different brands. The welding current was 110 A and a double V groove was made on each of the samples prior to welding. Welded samples were characterised by light microscope (LM). Charpy impact and hardness tests were conducted on base metal (BM), heat affected zone (HAZ) and weld zone (WZ). The results show that similar phase and microstructure morphology were formed in both joints. The total width of the brand (R) joint was 10.08 mm, while the brand (A) joint measured 13.23 mm. Brand (A) produced the hardest weld of 179 HV, as compared to the 170 HV weld of brand (R). However, brand (R) was reported to have a higher impact toughness of 130.30 J.

KEYWORDS: Brand, Zone, Weld, Electrode & Joint

Received: May 08, 2021; **Accepted:** May 28, 2021; **Published:** Jun 14, 2021; **Paper Id.:** IJMPERDAUG20216

1. INTRODUCTION

The welding process is one of the important joining techniques for metallic materials [1]. Welding is more economical, more convenient, and less susceptible to failure or corrosion when compared to other joining processes. Owing to the advantages of welding over other joining processes, numerous welding processes have been developed. As an industrial process, the cost of welding plays a crucial role in manufacturing decisions [2]. Welding – which is the most common permanent metal joining fabrication (machine parts and structures) process – is the joining of two similar metals by fusion, with or without the application of pressure and with or without the use of filler metal [3]. To achieve sound weld-integrity, along with enhanced service performance in welded carbon steel, having a selection of welding processes and parameters available is important [3]. Traditionally, mechanical components have been joined through fasteners and rivet joints and the like. In order to reduce manufacturing time, as well as achieve weight reduction and improvements in mechanical properties, a welding process is usually adopted [4]. The variety of different welding processes currently available means that welding is extensively used as a fabrication process for joining materials in a wide range of compositions, part shapes and sizes [4]. Before attempting to weld any material, it is essential to know how easy the material concerned is to weld and to be aware of any problems that might arise.

Up until the 19th century, one of the common types of welding process was forge welding, which was employed by blacksmiths to join iron and steel by way of heating the metal and hammering it [5]. After this decade

a new type of technology emerged that is arc welding and oxyfuel welding [5]. Steel is a metal alloy created from a mixture of iron and carbon. Iron is a key component in steel, while the carbon content varies between less than 0.2% and more than 0.5% mass, depending on the grade of steel [6]. Several different numbering systems have been developed for metals and alloys by various trade associations, professional engineering societies and standards organisations, as well as by concerns in private industry for their own use [7]. The welding of steels is affected by both temperature and the composition of the steel concerned, both of which extensively affect the evolution of the microstructure [6]. Materials joining and welding plays a key role in the economic development of a country. It is essential for the construction of highly sophisticated devices and structures, including vehicles, among others. [8].

Welded dissimilar metals have emerged as structural materials for various industrial applications, providing good combinations of mechanical properties such as strength and corrosion resistance, allied with lower cost [9]. Arc welding is currently used for the fabrication and construction of a variety of structures, such as buildings, bridges, ships, offshore structures, boilers, storage tanks, pressure vessels, pipelines, automobiles, and railroad vehicles [10]. Hardness is one of the most frequently measured properties of material. Its value helps to characterise resistance to deformation, densification and fracture [11]. Impact testing is a method used to determine the amount of energy absorbed by notched or un-notched samples of material during fracture [12].

The purpose of this paper is to compare the effects of welding electrode types of two different brands (brand A and brand R) on hardness, absorption energy and metallographic properties of mild steel.

2. MATERIAL

A rectangular plate of low carbon steel with thickness of 10 mm was used in this study as a base metal. Two different brands (A and R) of E6013 welding electrodes with diameter of 3.2 mm were used to join two rectangular plates of mild steel by using a shielded metal arc welding (SMAW) process and employing similar welding parameters. Spark emission spectroscopy was used to determine the chemical composition of base metal, and this information is presented in table 1.

Table 1: Chemical Composition of base Metal Material

ID Sample	C	Si	Mn	P	S	Cr	Ni	Mo	Al	Cu	Co	N	Fe
Base metal	0.166	0.026	0.503	0.009	0.006	0.168	0.018	0.007	0.047	0.050	0.006	0.015	98.933

3. METHODOLOGY

3.1 Welding Experiment

A Struers Discotom 60 cutting machine was used to cut rectangular plates of 75 mm x 50 mm x 10 mm using water cooling system. A single bevel-edged surfaces at a 45° angle was produced on a single edge of the plate by using a baby grinder for the butt weld joint, as illustrated in figure 1(a). The plate surfaces and edges were then cleaned with a wire brush prior to welding. A SMAW 160 trans-arc welding machine was used to make a butt weld joint between two plates (see figure 1 b). The welding parameters were kept constant during welding, i.e. welding current of 110 A, welding voltage of 220 V and a brand (A) electrode of 3.2 mm diameter. The two plates were welded together by building up welding beads until the V-grooves were filled with weld, as illustrated in Figure 1(b). The weld joints were tapped with a chipping hammer to remove the slag and to ensure that the gap was properly filled. The joints were then air cooled. The process was then repeated using different electrodes from brand (R).



Figure 1: (a) A Single V Groove Edge Bevel on Steel Plates, Indicated by the Black Arrows Pointing at the Edges, (b) A Butt Weld Joint of Two Steel Plates Made using E6013 Electrodes from Brand (A) and Brand (R).

3.2 Metallography

A cross-sectional area of the butt joint was cut from the welded plates and marked as samples A and R, according to the brand of electrode used. A sample preparation was performed by adopting the ASTM E03-1 standard. The samples were cut, mounted in plastic resin using a hot mount press at 180°C, and the mounts were cooled to room temperature using a water-cooling system. The mounts were planed and fine ground, followed by polishing sequences using a diamond lubricant until a 1 μ m surface finish was achieved. The surfaces were, thereafter, etched with 2% nital acid solution. The etched mounts were then examined and photographed under an Olympus DSX 50 Light Microscope. A weld profile micrograph at low magnification was acquired, as well a high-magnification micrograph of the base, HAZ and weld areas. The micrographs are presented and discussed in the results and discussion section.

3.3 Hardness Test

Hardness samples were cut in the following dimensions: 10 mm thickness, 10 mm width, and with a length of 98.3 mm. The samples are presented in figure 3. The samples were plane ground to ensure that the opposing surfaces were flat. The ASTM E384 test method was followed in this experiment. The instrument used for this test was an EMCO test machine using the Vickers hardness test method. Vertical lines were drawn on the samples which were 5 mm apart and are presented in Figure 2.

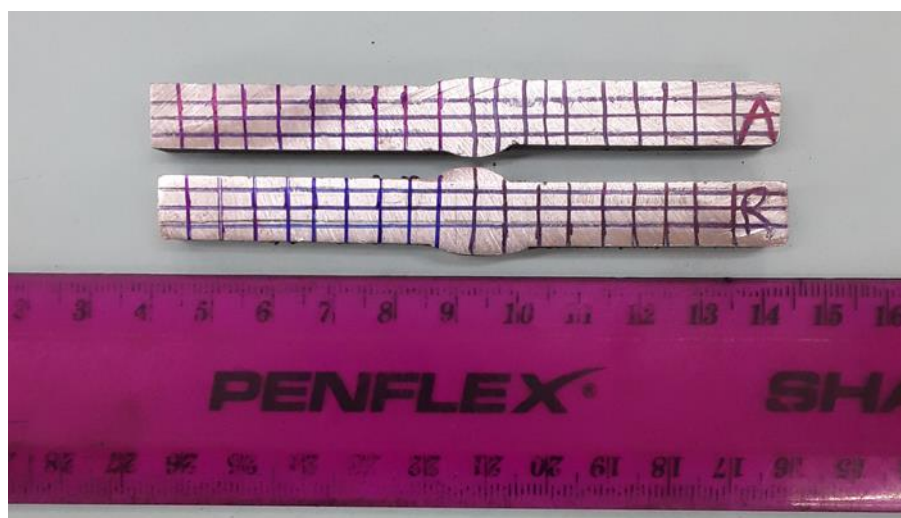


Figure 2: Hardness Samples with 5 mm Intervals Marked for Hardness Measurement.

Before the testing of welded samples took place, three tests were performed using a standard block sample for HV 30 to ensure that the machine readings were correct. For statistical consideration, three indentations were made from each vertical line. The test force used on this experiment was 30 kgf, while load holding time was 30 seconds in all cases. Test results were recorded and are presented in table 2.

Table 2: HV30 Hardness Comparison between Weld Joints of Brand (A) and Brand (R) Electrodes

Distance (mm)	Brand(A) Electrode (HV30)	Brand (R) Electrode (HV30)
0	145	152
5	145	153
10	146	153
15	146	159
20	150	170
25	157	168
30	179	170
35	160	160
40	154	157
45	152	154
50	152	152

3.4 Charpy V-Notched Impact Toughness Test

Welded samples were cut with a milling machine to the following dimensions: 55 mm x 10 mm x 10 mm. A V-notch groove, 2 mm deep, was machined at the centre of the butt weld joint using a milling machine. All sample dimensions were machined according to the ASTM E 23-12C standard [13]. Machined samples for the impact test are shown in figure 3.

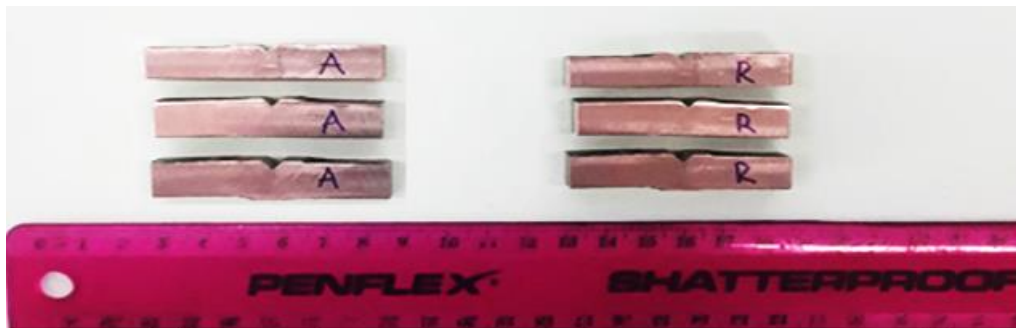


Figure 3: Charpy V-Notched Samples along with their Dimensions According to the ASTM E 23-12C Standard.

The impact test was performed in this study to determine the impact toughness of the butt weld joints made using E6013 electrodes of 3.2 mm diameter from both brand (A) and brand (R). This test was done to investigate the impact loading strength of butt weld joints produced using welding electrodes of different brands. All tests were carried out at room temperature (24°C) using an Instron 450J Charpy test machine. For statistical consideration, three samples were tested per welded plate and an average value was calculated. The results are shown in table 3 and are discussed in the results and discussion section.

Table 3: Weld Joint Impact Toughness of Different Brands

Number of Samples Tested	Sample (A) Impact Toughness (J)	Sample (R) Impact Toughness (J)
1	98.23	122.87
2	109.47	126.51
3	124.96	141.42
Average	110.89	130.27

4. RESULTS AND DISCUSSIONS

4.1 Macro and Micro Structures of SMAW Butt Weld Joints

A butt weld joint profile is presented in the cross-section macrograph at Figure 4 (a) of the sample welded using electrode R. This macrograph shows different zones of internal structures throughout the length of the joined plates. The butt weld profile entails three different zones, namely a base metal zone (BM), a heat affected zone (HAZ) and a weld zone (WZ). These zones were identified and marked as seen in Figure 4 (a). The differences in zones were induced by the variation of heating and cooling rates that took place during the welding process. The BM, which is adjacent to the HAZ, has a microstructure that is similar to that of the entire length and cross section of the welded plates, which means that the heat from the welding process did not affect or change the microstructures of the steel. Hence, the steel plates were preserved as processed microstructures condition. The HAZ contains microstructures that are different from those in the BM. This indicates that the heat input from welding changed the microstructures of the BM in the area adjacent to the weld, with the width of the area affected ranging between 2.52 mm to 2.75 mm. The WZ has distinctive microstructures from HAZ and BM. These structures originate from solidification of the molten electrode filler material during welding and produce a width of 4.81 mm.

However, the welded butt joint observed here has a continuous uniform phase structure with complete penetration of the joint and without any defects such as porosity or cracks. This makes it a defect-free weld, as shown in figure 4 (a).

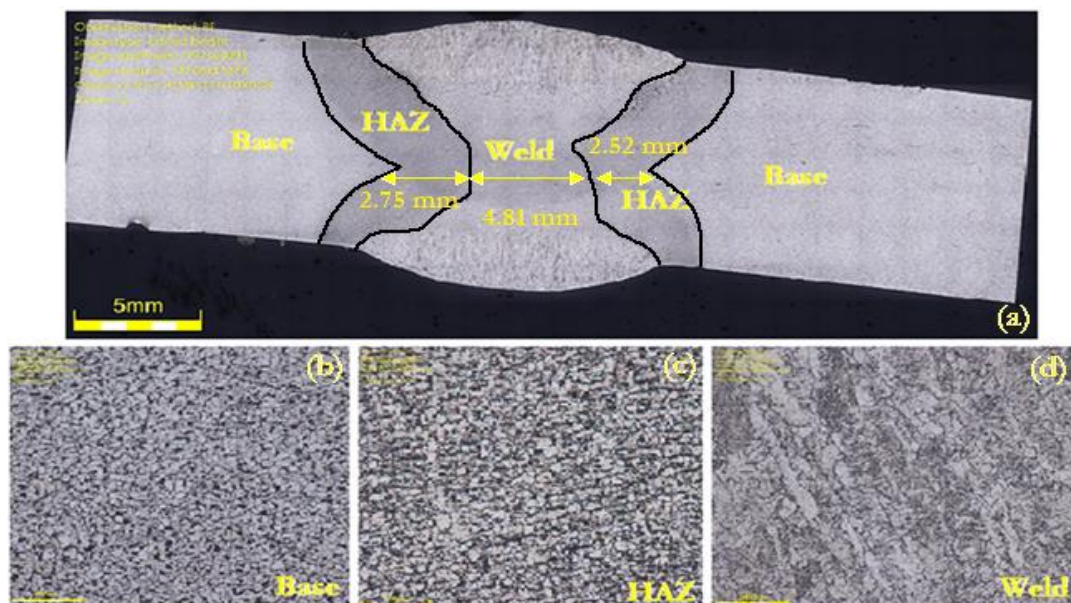


Figure 4: Micrographs of a Weld Joint made using a Brand (R) Electrode and showing (a) Weld Profile, (b) Base Metal (BM), (c) Heat Affected Zone (HAZ) and (d) Weld Zone (WZ).

Figure 4 (b) shows the microstructures of the BM, which are composed of grain structures (shape and size) that are fine and uniformly distributed across the matrix. The phases present are the ferrite (white) phase, present in large amounts, and the pearlite (black) phase, which exists in minute amounts. This means that the steel plate is ferritic steel. From the chemical composition of the BM, the 0.16% carbon content ranks the steel as low carbon and low alloy steel, which renders the matrix large volume of ferrite phase with pre-existing of pearlite phase in small volume. The grain morphology of the BM revealed the annealed condition of the steel plate, evident in the fine, equiaxed grain shape that is uniformly distributed. The HAZ has larger grain size compared to the BM, see Figure 4 (c) and Figure 4 (b) respectively. However, the phases that present in HAZ are similar, with even their volume fractions not differing much, as observed, except for the matter of grain coarsening. Heat input during welding increased the temperature of HAZ sufficiently to induce grain growth in the HAZ, leading to grain coarsening of microstructures in HAZ as compared with BM. The same results were reported by [14].

A weld zone (WZ), where material is melted during SMAW welding and subsequently rapidly cooled as a result of heat sink caused by cold solid BM edges, induced a quick transformation of molten metal into solid metal. The observed dendritic structures in WZ are similar to metal casting structures and are present in abundance in the WZ, as shown in Figure 4 (d) HAZ exhibits two different microstructures since it is subjected to different temperatures and cooling rates. Because of these different cooling rates, different phases were formed in the WZ, i.e. ferrites, Widmannstatten/acicular ferrite, bainite and pearlites phase.

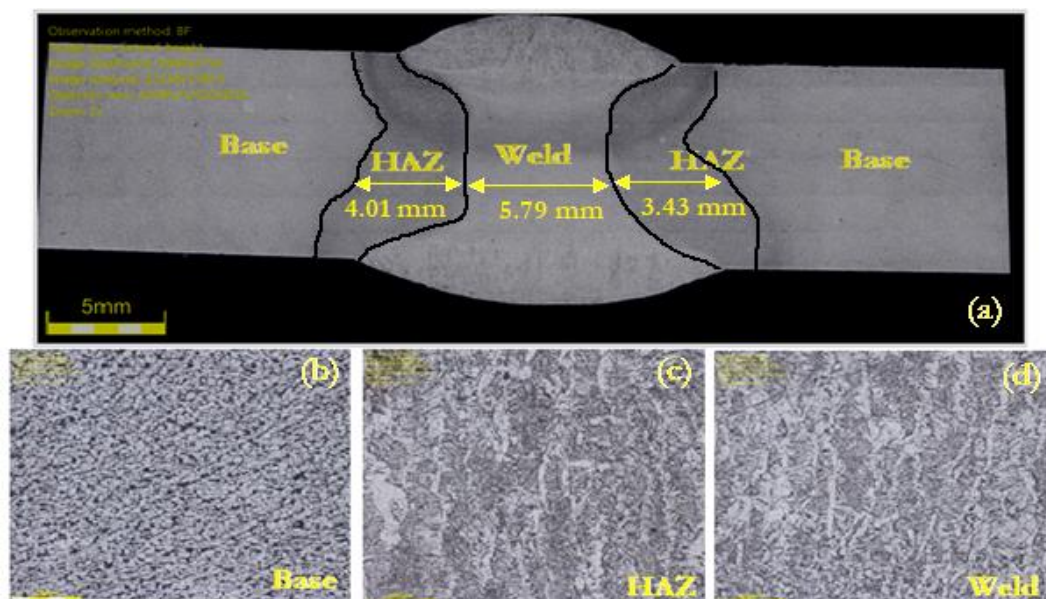


Figure 5: Micrographs of Weld Joint made using brand-A Electrode showing (a) Weld Profile, (b) Base Metal (BM), (c) Heat Affected Zone (HAZ) and (d) Weld Zone (WZ), Scale Bar of Small pic 200um.

Figure 5 (a) presents weld profile that was produced using a brand (A) electrode. It is observed that there are three different zones, these being the base metal (BM), the heat affected zone (HAZ) and the welded zone (WZ), as was observed in the previous weld. From Figures 4 and 5, it is noted that HAZ formed a double V-shape and that the weld filled the double V-groove which was made prior to joining the two plates using the SMAW welding process. The width of HAZ ranges between 3.43 mm and 4.01 mm, which appears to be wider than the HAZ width using the brand R electrode. The WZ has a width of 5.79 mm, which is greater than what was measured using the brand R electrode. These differences

affect the impact strength of the joint.

Figure 5 (b) presents the same observation that was made on Figure 4 (b), where the microstructures of BM were not affected during material welding. These indicate that the area was not affected by the heat input of the welding. The grain structures have well defined structure (shape and size), with finer and more homogeneous distribution across the matrix, as seen in Figure 5 (b). However, a HAZ has a noticeable large grain size when compared to the grain size of a BM, which reveals grain growth as a result of high temperatures and slow cooling rate during and after welding, see Figure 5 (c). Surprisingly, the WZ microstructures show similar grain formation to that observed in HAZ. This observation makes for a striking difference between this and the WZ made by electrode R, as seen in Figure 4 (c). These zones, namely HAZ and WZ entailed Widmannstatten/acyclic ferrite and cementite in the form of pearlite, bainite and ferrite phases. Their formation is mainly controlled by different cooling rates. Although chemical composition might have been an influence here, this would be insignificant since the plates were made of same grade of steel and had a similar electrode grade. The only difference here was the brand name. The Widmannstatten/acyclic ferrite and bainite in the form of pearlite are considered to be hard and brittle phases as compared to ferrite and pearlite phases.

Other factors that might have contributed to higher temperatures during welding might be the gap between the electrode and the material, the welding speed and stoppage caused by the replacing of a length of electrode when this ran out, resulting in different heating and cooling rates in HAZ and WZ and thus creating the different microstructures which were noticed in Figure 5 (c) and 5 (d). It is known that the microstructures depend primarily on the chemical composition and cooling rate [15]. The Widmannstatten ferrite and bainite phases were formed due to the fast cooling rates of the high temperature weld. The same results were reported in the study on “Understanding the effect of weld parameters on the microstructures and mechanical properties in dissimilar steel welds” [16].

4.2 Hardness

The hardness results from table 2 are graphically presented in figure 6. The figure depicts two graphs that present the Vickers hardness 30KGF (HV 30) profile of two weld joints produced from electrodes of brand (A) (black curve) and brand (R) (blue curve).

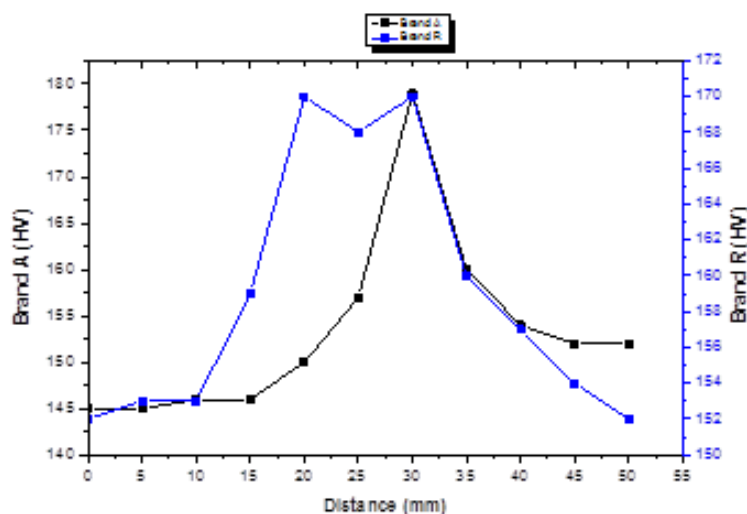


Figure 6: A Graph of Profile Hardness HV30 for Brand (A) (Black Curve) and Brand (R) (Blue curve) Joint Measured from base Metal to the Centre of Weld.

It was noted that both graphs map out similar hardness profiles in which hardness begins to increase gradually with increase in distance when approaching the HAZ region and that hardness reached its peak at the weld zone and decreased further away from weld. In addition, HAZ, by increasing the distance, may be seen in the figure. This type of hardness profile is normally expected in a welded joint, especially when post-weld heat treatment is not applied to homogenise the microstructure of the HAZ and weld zone with the base metal.

From observation of the microstructures, it was noticed that different phases, as well inhomogeneity of grain morphologies, had formed through the weld spans during welding. The base metal zone revealed a large volume ferrite phase with patches of pearlite phase, both having a structure typical of equiaxed grains. While HAZ and weld metal show a mixture of Widmannstatten ferrite, bainite and pearlite phases in different amounts, their structure appears to be dendrites. It is known that the ferrite phase has lower hardness than Widmannstatten ferrite, followed by the pearlite and then bainite phase, while grain dendrite structures are harder than the equiaxed structures. This may explain the hardness profile that was observed on both welds. However, a HAZ of brand (A) shows higher hardness than a HAZ of brand (R), but the welds have approximately equal hardness. The hardness curve of brand (R) has shifted forward as compared with hardness curve of brand (A), meaning that the width of the HAZ + weld of brand (A) (13.23 mm) is greater than the width of brand (R) (10.08 mm). This implies that the heat input produced during welding using brand (A) was greater than the heat input of the brand (R) electrode because the heat-affected area of base metal microstructures was wider than that of brand (R), as can be seen in figure 4 (which refers to brand (R) microstructures) and in figure 5 (which refers to brand (A) microstructures). This explains why the hardness of curve A increases earlier than that of curve R, as seen in figure 6.

4.3 Charpy V-Notched Impact Toughness

The impact toughness results of both electrode brands – (A) and (R) – are presented in a bar chart in figure 7. The bar chart shows that weld produced using brand (R) has the ability to absorb a greater amount of impact loading than the weld produced using brand (A). This implies that the brand (R) weld has great impact resistance or impact toughness than weld A, as seen in figure 7.

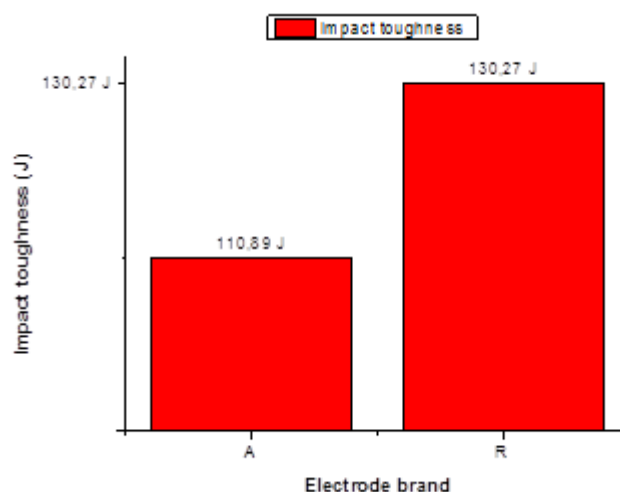


Figure 7: Impact Toughness of Electrode Brand (A) vs Brand (R).

This could be attributed to the microstructures formed during welding of the plates. It is known that increases in the property of hardness occur at the expense of the toughness property of the material concerned. The hardness and microstructures profiles observed above justify the observed toughness property in the two different welds. The hardness of the brand (A) weld is higher and covers a wider area of the joint as compared with the narrow, higher hardness zone of the brand (R) weld. During impact testing, the notch was made at the centre of the joint and both 2mm wider and deeper. This implies that the impact loading was concentrated at the centre of the joint by means of using a notch. The wider area of the brand (A) joint has weaker impact strength as compared with narrow area of the brand (A) joint, this being due to their hardness profile, as observed in figure 6. This behaviour is attributed to the microstructures formed during welding of two joints where Widmannstatten/acicular ferrite and bainite phases are considered to be hard phases. As compared with the ferrite phase, it was noticed that a wider area of joint was dominated by hard phases and that these have a dendrite structure. This has a negative effect on the impact strength of the material when compared with joint of brand (R), which has a narrow area of these hard phases.

5. CONCLUSIONS

The study of effects of two different brands of electrode E6013, brand (A) and brand (R), under SMAW on the mechanical properties of joints reveals that:

- Similar phase and microstructure morphologies were formed in both joints
- The total width of the brand (R) joint was 10.08 mm, while the total width of the brand A joint was 13.23 mm.
- Both electrodes revealed similar hardness profiles, with a maximum hardness of 179 HV 30 for brand (A) and of 170 HV 30 for brand (R).
- A joint created with a brand (R) electrode has higher impact toughness (at 130.27 J) than joint created with brand (A) (at 110.89 J), both at room temperature.
- It was observed that E6013 electrodes, both with a tip diameter of 3.2 mm, but from different brands, affected the mechanical properties of 10 mm thick mild steel plates differently when these were welded using the shielded metal arc welding (SMAW) process.

REFERENCES

1. S. B. Jamaludin, M. N. Mazlee, S. K. A. Kadir, and K. R. Ahmad, "Mechanical properties of dissimilar welds between stainless steel and mild steel," *Adv. Mater. Res.*, vol. 795, no. September, pp. 74–77, 2013.
2. Bade Venkata Suresh, P. Srinivasa Rao, Potnuru Govinda Rao, "Influence of Flexural Strength on Welded Joints under the Effect of Electrode Vibratory Welding Process", *International Journal of Mechanical and Production Engineering Research and Development (IJMPERD)*, Vol. 10, Issue 3, pp, 1345–1352
3. R. A. Mohammed, M. Abdulwahab, and E. T. Dauda, "Properties evaluation of shielded metal arc welded medium carbon steel material.," *Int. J. Innov. Res. Sci. Eng. Technol.*, vol. 2, no. 8, pp. 3351–3357, 2013.
4. I. Harish, Santosh Patro & P Srinivasa Rao, "Parametric Optimization of Machining Parameters by using Coated Copper 1487 Wire Electrode on Wire Electric Discharge Machining", *International Journal of Mechanical and Production Engineering Research and Development (IJMPERD)*, Vol. 10, Issue 3, pp, 1485-1498

5. O. S. Odebiyi, S. M. Adedayo, L. A. Tunji, and M. O. Onuorah, "A review of weldability of carbon steel in arc-based welding processes," *Cogent Eng.*, vol. 6, no. 1, 2019.
6. Walaa A. Hussein, Amal S. I. Ahmed, Wafaa A. Ghanem & Ghalia A. Gaber, "Electrochemical Corrosion Behavior of Cu-Zn Alloys in Oxy-Acid Solution", *IASET: International Journal of Metallurgical, Materials and Chemical Engineering (IASET: IJMMCE)*, Vol. 1, Issue 1, pp; 41-46
7. S. I. Talabi, O. B. Owolabi, J. A. Adebisi, and T. Yahaya, "Effect of welding variables on mechanical properties of low carbon steel welded joint," *Adv. Prod. Eng. Manag.*, vol. 9, no. 4, pp. 181–186, 2014.
8. S. C. Goud, "Effect of Welding on Mild Steel Material on Its Microstructure and Properties," *Adv. Res. Sci. Eng.*, vol. 5, no. 08, pp. 256–260, 2016.
9. Bishnu M Jha & A Mandal, "Overcut and Profile of the Machined Features in Electrochemical Machining ", *IASET: International Journal of Metallurgical, Materials and Chemical Engineering (IASET: IJMMCE)*, Vol. 1, Issue 1, pp; 29-40
10. S. Ragu Nathan, V. Balasubramanian, S. Malarvizhi, and A. G. Rao, "Effect of welding processes on mechanical and microstructural characteristics of high strength low alloy naval grade steel joints," *Def. Technol.*, vol. 11, no. 3, pp. 308–317, 2015.
11. ClassNK, "Technical Information Technical Information," *Lemn. public Light.*, vol. 1, no. 0715, pp. 1–6, 1998.
12. P. K. Halder, N. Paul, and S. Rahman, "Effect of welding on the properties of Mild steel & cast iron specimen," *Int. Conf. Mech. Ind. Energy Eng.*, no. May, pp. 3–7, 2013.
13. I. O. Oladele, O. T. Betiku, A. M. Okoro, and O. Eghonghon, "Microstructure and Mechanical Properties of 304L and Mild Steel Plates Dissimilar Metal Weld Joint," *Acta Tech. Corviniensis-Bulletin Eng.*, vol. 11, no. 2, pp. 77–81, 2018.
14. K. Shinagawa, "Arc Welding of Specific Steels and Cast Irons," *Arc Weld. Specif. Steels Cast Irons*, pp. 2–22, 2015.
15. G. D. Quinn, "Indentation Hardness Testing of Ceramics," *Mech. Test. Eval.*, no. February, pp. 244–251, 2018.
16. N. Navaranjan and T. Neitzert, "Impact Strength of Natural Fibre Composites Measured by Different Test Methods: A Review," in *MATEC Web of Conferences*, 2017, vol. 109.
17. ASTM E 23-12c, "Standard Test Methods for Notched Bar Impact Testing of Metallic Materials," *Standards*, vol. i, pp. 1–25, 2013.
18. V. Bhavar et al., "Effect of post weld heat treatments (PWHTs) on electron beam welded SAE 5137 Steel," *ASM Int. - 29th Heat Treat. Soc. Conf. HEAT TREAT 2017*, vol. 2017-Octob, no. October, pp. 511–518, 2017.
19. P. J. Prajapati and V. J. Badheka, "Investigation on three different weldments on performance of SA516 Gr70 steel material," *Alexandria Eng. J.*, vol. 58, no. 2, pp. 637–646, 2019.
20. D. K. Singh, V. Sharma, R. Basu, and M. Eskandari, "Understanding the effect of weld parameters on the microstructures and mechanical properties in dissimilar steel welds Understanding the effect of weld parameters on the microstructures mechanical properties in di," *Sci. Sci. Sci. Manuf.*, vol. 35, pp. 986–991, 2019.
21. Husaini et.al, "Effects of welding on the change of microstructure and mechanical properties of low carbon steel Effects of welding on the change of microstructure and mechanical properties of low carbon steel," in *The 8th Annual International Conference (AIC) 2018 on Science and Engineering*, 2019, pp. 1–9.
22. W. Zhou and K. G. Chew, "Effect of welding on impact toughness of butt-joints in a titanium alloy," *Mater. Sci. Eng.*, vol. 347, no. 1–2, pp. 180–185, 2003.